Actomyosin contraction in follicular epithelium provides the major mechanical force for follicle rupture during *Drosophila* ovulation

Stella E. Cho[1], Wei Li[1#], Andrew M. Beard[1], Jonathan A. Jackson[3, 4!], Risa Kiernan[1], Kazunori Hoshino[5], Adam C. Martin[3], and Jianjun Sun[1,2*]

1 Department of Physiology & Neurobiology, University of Connecticut, Storrs, CT 06269, USA
2 Institute for Systems Genomics, University of Connecticut, Storrs, CT 06269, USA
3 Department of Biology, Massachusetts Institute of Technology, Cambridge, MA 02139, USA
4 Graduate Program in Biophysics, Harvard University, Boston, MA 02115, USA
5 Department of Biomedical Engineering, University of Connecticut, Storrs, CT 06269, USA

Current address: Foundation Medicine Inc., Cambridge, MA 02141, USA
! Current address: Max Planck Institute of Molecular Cell Biology and Genetics, Pfotenhauerstraße 108, Dresden 01307, Germany

*** Corresponding Author**

Dr. Jianjun Sun
Tel. 860-486-4666
Fax. 860-486-3303
Email: jianjun.sun@uconn.edu

Running title: actomyosin in follicle rupture

Keywords: Ovulation, follicle rupture, actomyosin contraction, mechanical force, Rho1, ROK

Abstract

Ovulation is critical for sexual reproduction and consists of the process of liberating fertilizable oocytes from their somatic follicle capsules, also known as follicle rupture. The mechanical force for oocyte expulsion is largely unknown in many species. Our previous work demonstrated that *Drosophila* ovulation, as in mammals, requires the proteolytic degradation of the posterior follicle wall and follicle rupture to release the mature oocyte from a layer of somatic follicle cells. Here, we identified actomyosin contraction in somatic follicle cells as the major mechanical force for follicle rupture. F-actin and non-muscle myosin II (NMII) are highly enriched in the cortex of follicle cells upon stimulation with octopamine (OA), a monoamine critical for *Drosophila* ovulation. Pharmacological disruption of F-actin polymerization prevented follicle rupture without interfering with the follicle wall breakdown. In addition, we demonstrated that OA induces Rho1 GTPase activation in the follicle cell cortex, which activates Rho kinase (ROK) to promote actomyosin contraction and follicle rupture. All these results led us to conclude that octopamine signaling induces actomyosin cortex enrichment and contractility, which generates the mechanical force for follicle rupture during *Drosophila* ovulation. Due to the conserved nature of actomyosin contraction, this work could shed light on the mechanical force required for follicle rupture in other species including humans.

Significance Statement

Ovulation is the process of the expulsion of mature oocytes out of the follicle capsule. It is largely unknown what mechanical force is required for pushing the oocyte out. In this study, we investigated the force required for *Drosophila* ovulation and identified that the actomyosin network generates the major mechanical force for the expulsion of *Drosophila* oocytes from mature follicles. The actomyosin network, which is highly conserved and known to produce mechanical force for many biological processes at both cellular and tissue scales, is greatly enriched in the cortex of follicular epithelium and is activated by Rho1 GTPase to generate mechanical force during ovulation. Due to its conserved nature, this mechanism may be applied to ovulation in other species.

Introduction

Ovulation is a complex reproductive process that ends with the rupture of the mature follicle and the expulsion of the fertilizable oocyte. In mammals, ovulation is induced by a surge of luteinizing hormone (LH) secreted by the pituitary gland, which mediates a complex signaling network involving progesterone and prostaglandin signaling in mature follicles and ultimately activates proteolytic enzymes at the apex of mature follicles for follicle rupture to occur (1–3). In addition, LH activates endothelin signaling to increase the contractile activity of smooth muscle cells in the theca layer of the mature follicles, which is also critical for follicle rupture and potentially provides the mechanical force for the expulsion of the oocyte via increasing intrafollicular pressure (4–11). Recent work also showed that LH induces cytoskeletal shape changes and inward migration of granulosa cells, but the role of such changes for follicle rupture

68 is still unclear (12–16). Despite these studies, the mechanical force for follicle rupture and
69 expulsion of oocytes has never been fully elucidated and remains as an underexplored area in the
70 ovulation field (17, 18).
71 Recent advancements in *Drosophila* ovulation make *Drosophila* as an attractive model
72 for the study of ovulation mechanisms (19). A *Drosophila* follicle develops through 14
73 morphologically distinct stages to become a mature (stage-14) follicle, which consists of an
74 oocyte wrapped by a thin layer of somatic follicle cells (20), that is ready for ovulation.
75 *Drosophila* ovulation is induced by octopamine (OA) signaling, equivalent to adrenergic
76 signaling in mammals (21), from the nerves innervated with the ovaries (22–25). OA activates
77 the Octopamine receptor in mushroom body (OAMB) in mature follicle cells, leading to the
78 activation of matrix metalloproteinase 2 (MMP2) for the breakdown of the follicle wall at the
79 posterior region, and NADPH oxidase (NOX) in all follicle cells for reactive oxygen species
80 (ROS) production, ultimately causing follicle rupture (26–28). In addition, OA signaling
81 regulates ovarian and oviduct muscle contraction, which is also important for the success of
82 *Drosophila* ovulation (29–33). However, it is questionable whether the muscle contraction
83 provides the major mechanical force for follicle rupture, since the entire follicle rupture can be
84 recapitulated *ex vivo* using isolated mature follicles without any muscle sheaths (26). During
85 follicle rupture, the entire layer of follicle cells is compressed towards the anterior dorsal
86 appendage after the breakdown of the posterior follicle wall by MMP2 (26, 27). Therefore, the
87 mechanical force for the compression of follicle cells and expulsion of the oocyte during follicle
88 rupture is obscure.
89 The actomyosin cytoskeleton is highly conserved among various species and crucial for
90 generating the mechanical force for biological processes ranging from the subcellular to the

tissue level, including endocytosis, cytokinesis, cell migration, tissue morphogenesis (34–37). The structural composition of the actomyosin networks primarily consists of the scaffold of filamentous actin (F-actin) and the motor protein, myosin II, which binds and slides F-actin within a cortical network to generate contractility (35, 38). Non-muscle myosin II (NMII) in epithelial tissues typically forms mini filaments, which is composed of two heavy chains, two essential light chains, and two regulatory light chains (encoded by *spaghetti squash, sqh* in *Drosophila;* 34, 39). The phosphorylation of the regulatory light chain at highly conserved residues (Thr18 and Ser19 in mammals, Thr20 and Ser21 in *Drosophila*) is critical for NMII activation and regulated by various kinases including Rho kinase [ROK in *Drosophila* and ROCK in mammals; (40–43)]. ROK is activated by small GTPase Rho1, which also activates the formin-family protein Diaphanous (Dia) to promote actin polymerization (44). Therefore, Rho1 plays important roles for the generation of actomyosin contractile force during tissue morphogenesis (34, 45). In *Drosophila*, the Rho1-ROK-actomyosin contraction has been comprehensively studied in wound healing to understand epithelial morphogenesis, and in many developmental processes such as gastrulation during embryogenesis, specifically mesoderm or endoderm invagination and germ-band extension (42, 46, 47). In addition, actomyosin contraction is crucial for several processes in *Drosophila* oogenesis, such as border cell migration(48–51), nurse cell dumping (41, 52, 53) and egg elongation (45, 54–56). However, its role in ovulation has never been elucidated.

In this study we discovered that pharmacological inhibition of actomyosin, but not the microtubule network, prevented the OA-induced follicle rupture. We also showed that F-actin, NMII, and active Rho1 were highly enriched in the cortex of follicle cells when mature follicles were stimulated with OA. Further genetic and pharmacological experiments demonstrated that

OA/OAMB activates Rho1-ROK-actomyosin contraction to generate the mechanical force, which leads to the compression of the follicle cell layer and the expulsion of the oocyte during follicle rupture. Therefore, our work shed light on the mechanical force required for follicle rupture during *Drosophila* ovulation, and similar mechanisms could be involved in ovulation in other organisms.

Results

OA-induced oocyte rehydration is not required for follicle rupture

During ovulation, octopamine (OA) signaling triggers the breakdown of posterior follicle cells and the release of the encapsulated oocyte, while the remaining follicle cells collapse to form a corpus luteum that potentially produces steroid hormones (27). This entire follicle rupture process can be recapitulated *in vitro* by culturing intact mature follicles deprived of muscle sheath in OA medium (26). At the end of the rupture process, all follicle cells are highly compacted at the dorsal appendage region (Fig. 1A). To quantify this tissue morphogenesis, we measured the anterior-posterior axis length of the follicle cell layer before and after rupture and calculated the ratio of this compression. It showed that the follicle cell layer had a 3.6-fold compression in the anterior-posterior axis after follicle rupture (Fig. 1B-C). This suggests the existence of a mechanical force for inducing follicle cell layer compression; yet the nature of this mechanical force for follicle rupture remains unknown.

Previous works have demonstrated oocyte dehydration in mature follicles and subsequent rehydration after ovulation for egg activation (57). We also observed that oocytes rehydrate after the exposure to OA in our *ex vivo* culture system. Mature follicles without OA exposure showed

136 a dehydrated morphology with a dented surface (Fig. 1D and Movie S1). In contrast, within 15
137 minutes of OA exposure even before follicle rupture, mature follicles showed no obvious dented
138 surface (Fig. 1E and Movie S2). Therefore, we hypothesized that oocyte rehydration could
139 potentially create tension against the follicle cell layer, which may lead to the follicle cell layer
140 retraction anteriorly once the posterior follicle cells are broken after OA stimulation. To test this
141 hypothesis, we precisely measured the volume of mature follicles before and after OA exposure.
142 A steady increase in volume was observed in mature follicles after OA exposure, while those
143 without OA exposure showed less volume increase if any (Fig. 1G-H). In addition, mature
144 follicles in a hypertonic medium with 400 mM sucrose did not increase in volume even with OA
145 exposure, indicating that the hypertonic medium prevented follicle rehydration (Fig. 1F-H and
146 Movie S3). Next, we examined follicle rupture in both control and hypertonic media. To our
147 surprise, mature follicles in the hypertonic medium ruptured at a similar rate to those in the
148 control medium after OA treatment (Fig. 1I-K). This indicates that oocyte rehydration is unlikely
149 to provide the major mechanical force for follicle rupture in *Drosophila*.
150
151 **The mechanical force driving follicle rupture is actin-mediated**
152 To elucidate the nature of the mechanical force required for follicle rupture, we
153 investigated the cytoskeleton system, known to generate force in many biological processes. We
154 pharmacologically inhibited actin- or microtubule-mediated mechanical force in mature follicles
155 and examined their impact on OA-induced follicle rupture. Colchicine and nocodazole were
156 employed to inhibit microtubule elongation, and cytochalasin D and latrunculin A were used to
157 disrupt actin dynamics. Intriguingly, both colchicine- and nocodazole-treated follicles ruptured

158 normally after OA stimulation; however, both cytochalasin D and latrunculin A at 1 μg/ml
159 severely inhibited OA-induced follicle rupture (Fig. 2A-G and SI Appendix, Fig. S1A-C).
160 Considering the essential roles of MMP2 and superoxide production in OA-induced
161 follicle rupture (27, 28), we tested whether cytochalasin D and latrunculin A inhibit OA-induced
162 MMP2 activity or superoxide production. Using an *in situ* zymography assay previously
163 developed for examining MMP2 activity (26), we found that 85% of mature follicles in the
164 control medium showed MMP2 activity at the posterior end of mature follicles after OA
165 stimulation, while cytochalasin D and latrunculin A treatment showed no significant difference
166 of OA-induced MMP2 activity (Fig. 2H-L). This result demonstrates that both drugs did not
167 inhibit OA-induced MMP2 activation. Additionally, we measured the OA-induced superoxide
168 production in mature follicles treated with control, cytochalasin D, or latrunculin A using a
169 luminescent assay we developed previously (28). Cytochalasin D-treated follicles did not show
170 any effect on superoxide production, while latrunculin A-treated ones had a slightly reduced
171 production about 30 minutes after OA stimulation (Fig. 2M and SI Appendix, Fig. S1D). This
172 delayed reduction of superoxide production by latrunculin A treatment could be due to the
173 indirect effect from the disrupted actin dynamics such as Oamb receptor recycling. Nonetheless,
174 these findings collectively suggest that cytochalasin D and latrunculin A treatment does not
175 cause acute toxicity or impact OA-induced MMP2 activation and superoxide production. This
176 work also leads us to hypothesize that actin-mediated mechanical force may play important roles
177 in follicle rupture, independent of MMP2 activity and superoxide production.
178

OA/OAMB signaling induces actomyosin cortex enrichment in main-body follicle cells before follicle rupture

The actomyosin contractile force serves various roles in numerous biological processes (34, 35, 54). To demonstrate whether actomyosin plays a role in follicle rupture, we initially examined the distribution of filamentous actin (F-actin) and non-muscle myosin II (NMII) in follicle cells with or without OA stimulation. In the absence of OA, a low level of F-actin was localized both in the cytoplasm and along the cortex of follicle cells in mature follicles (Fig. 3A). The incubation period of up to 45 min did not cause any drastic changes in the distribution of F-actin (Fig. 3A-B, 3D and SI Appendix, Fig. S2A-B). However, when mature follicles were treated with OA, a notable enrichment of F-actin occurred in the cortex of the main-body follicle cells, existing along most of the lateral cell membrane (Fig. 3C-D and SI Appendix, Fig. S2C-D). Detailed mapping of subregions along the lateral membrane was challenging due to the squamous nature of these follicle cells at stage 14. Subsequently, we tested whether NMII, the working partner of F-actin, is also enriched at the follicle cell cortex after OA stimulation. Using a reporter for the regulatory light chain of NMII, *sqh::GFP*, we observed a significant enrichment of NMII in the cortex of the main-body follicle cells after OA treatment (Fig. 3E-H and SI Appendix, Fig. S2F-I), mirroring the F-actin distribution. Notably, the intensity levels of both F-actin and NMII reached a plateau around 30 minutes after OA treatment (Fig. 3D and 3H).

During the analysis, we noticed weaker intensity of F-actin and NMII in posterior follicle cells compared to main-body follicle cells after OA stimulation (Fig. 3C and 3G). To characterize this further, we quantified the intensity of F-actin and NMII in posterior follicle

cells and compared to those in main-body follicle cells after a 30-minute culture with or without OA. Without OA treatment, F-actin was lower in the cortex of main-body follicle cells than posterior follicle cells; in contrast, with OA, F-actin was slightly higher in the cortex of main-body follicle cells than posterior follicle cells (SI Appendix, Fig. S2E). Moreover, the cortex NMII was more than two-fold higher in main-body follicle cells than in the posterior follicle cells after OA stimulation (SI Appendix, Fig. S2J). These findings suggest that OA induces actomyosin enrichment primarily in the cortex of main-body follicle cells, prompting our subsequent analyses focusing on main-body follicle cells.

Next, we tested whether the OA-induced actomyosin cortex enrichment is mediated by OAMB, the receptor required for OA-induced follicle rupture (26). We isolated mature follicles from *oamb* mutant female ovaries and measured F-actin and NMII signal after a 30-minute culture with or without OA stimulation. Compared to the control, *oamb* mutant follicle cells showed a significant reduction in cortex enrichment of both F-actin and NMII after OA stimulation (Fig. 3I-N). Altogether, these results indicate that OA/OAMB signaling induces actomyosin cortex enrichment in main-body follicle cells before follicle rupture.

This redistribution of actomyosin after OA stimulation supports our hypothesis that actomyosin contraction provides the mechanical force for follicle rupture. To further confirm this, we also examined the distribution of F-actin and NMII in follicles treated with cytochalasin D and latrunculin A, both of which efficiently inhibited follicle rupture. As expected, both cytochalasin D and latrunculin A disrupted the proper cortex enrichment of actomyosin (SI Appendix, Fig. S3). These results validate the efficiency of the drugs and simultaneously support the hypothesis that actomyosin enrichment in follicle cell cortex is required for follicle rupture.

ROK regulates actomyosin contraction and is required for follicle rupture.

In order to test whether cortex-enriched actomyosin generates contractile force in follicle cells for follicle rupture, we aimed to disrupt ROK activity, a crucial factor for Sqh phosphorylation and NMII contractility (41, 58). Using an antibody against monophosphorylated Sqh at Ser-21 [Sqh-1P; (59)], we observed significant cortex enrichment of Sqh-1P after OA stimulation (Fig. 4A-B). In contrast, mature follicles treated with the well-known ROK inhibitor Y-27632 (60) resulted in the complete elimination of Sqh-1P in mature follicle cells after OA stimulation (Fig. 4C-D). In addition, Y-27632-treated follicles showed a reduced level of overall Sqh cortex enrichment as anticipated (Fig. 4E-H and SI Appendix, Fig. S4A). However, F-actin remained enriched in the cortex of follicle cells even after Y-27632 treatment (Fig. 4I-L and SI Appendix, Fig. S4B). We noticed that F-actin accumulates more at tri- and bi-cellular junctions in Y-27632 treated follicles, consistent with the idea that ROK regulates the stability of actin through α-catenin at the cell-cell junctions (61). Therefore, Y-27632 treatment yielded a less uniform cortex enrichment of F-actin, as expected.

To determine whether Y-27632 indeed disrupts the actomyosin contractility in mature follicle cells after OA stimulation, we performed the laser ablation experiment (62) to observe the tension of the follicle cells with or without Y-27632 treatment. In control follicles after a 30-minute OA stimulation, a small laser cut on the cortex of the main-body follicle cells led to a quick expansion of the lesion site (Fig. 4M-O and Movie S4). In contrast, in Y-27632-treated follicles after a 30-minutes OA stimulation, laser cut did not result in an expansion of the lesion site (Fig. 4P-R and Movie S5). We measured the initial recoil velocity of Sqh::GFP around the

ablation site after the cut, which is proportional to actomyosin tension. The Y-27632-treated follicle cells exhibited a negative recoil velocity close to 0 μm/sec, compared to 0.12 μm/sec in control follicle cells (SI Appendix, Fig. 4S). This data supports that OA-induced actomyosin contraction can be inhibited by the ROK inhibitor Y-27632.

Finally, we investigated whether ROK inhibition by Y-27632 is sufficient to block OA-induced follicle rupture. Consistent with our hypothesis, Y-27632 was sufficient to inhibit OA-induced follicle rupture in a dose-dependent manner (Fig. 4T-V). We also observed the breakdown of posterior follicle cells in Y-27632-treated follicles, indicating that Y-27632 does not inhibit OA-induced MMP2 activity (Fig. 4U). Lastly, we also attempted to knock down *rok* in follicle cells using RNA interference (RNAi). Unfortunately, both RNAi lines failed to prevent Sqh-1P cortex enrichment (SI Appendix, Fig. S5A-F), indicating an ineffective knockdown of *rok* in mature follicle cells. Consistent with this, mature follicles from *rok* RNAi females showed normal OA-induced follicle rupture (Fig. S5G). Although *rok* RNAi females laid fewer eggs than control females, they showed no statistical difference in terms of ovulation time (Fig. S5H-I), indicating no ovulation defect *in vivo*. Nevertheless, our pharmacological data suggest that ROK is required for OA-induced actomyosin contraction and follicle rupture.

OA/OAMB signaling induces Rho1 activation at the follicle cell cortex

The involvement of ROK in follicle rupture prompted us to hypothesize that its upstream regulator, Rho1 GTPase, is also involved in the actomyosin contraction and follicle rupture. To test this hypothesis, we first examined whether OA induces Rho1 activation at the cortex of the follicle cells, where F-actin and NMII are enriched. For this purpose, we utilized an active Rho1

sensor, Ani-RBD::GFP, in which Rho1-binding domain (RBD) from Anillin is fused with GFP (63). The active Rho1 (Rho1-GTP) can bind to Ani-RBD::GFP, which is reflected by the GFP pattern inside the cells. Consistent with our hypothesis, we found that Ani-RBD::GFP was distributed in the cytoplasm without OA stimulation but quickly redistributed to the cortex of the main-body follicle cells after OA stimulation, which indicates an increased activation of Rho1 at the cortex of main-body follicle cells induced by OA (Fig. 5A-B and SI Appendix, Fig. S6A-H). Following a 30-minute OA stimulation, 86% of mature follicles exhibited active Rho1 at the follicle cell cortex (Fig. 5C). It is worth to note that posterior follicle cells did not display prominent Rho1 activation at the follicle cell cortex after OA stimulation (Fig. 5B).

Next, to determine whether OA-induced Rho1 activation at the follicle cell cortex also depends on OAMB, we examined the Rho1 sensor in *oamb* mutant mature follicles after a 30-minute OA stimulation. We measured the intensity of Ani-RBD::GFP (Rho1-GTP) in the main-body follicle cells after a 30-min culture with or without OA stimulation. The *oamb* mutant follicles showed significant reduction in cortex Rho1 activity after OA stimulation in comparison to control follicles (Fig. 5D-H). Consistent with this, *oamb* mutant follicles also showed significant reduction in cortex Sqh-1P after OA stimulation (SI Appendix, Fig. S5J-N). Altogether, these data suggest that OA/OAMB signaling induces Rho1, and subsequent ROK, activation at the follicle cell cortex before follicle rupture.

Rho1 is required and sufficient for follicle rupture/ovulation

To determine the role of active Rho1 in mature follicles, we first overexpressed a dominant-negative (DN) form of *Rho1* (*Rho1*^{DN}) in mature follicle cells using *47A04-Gal4* driver

289 and examined its effect on the cortex enrichment of actomyosin. As anticipated, overexpression
290 of *Rho1*^{DN} in mature follicle cells impeded the OA-induced F-actin enrichment (Fig. 6A-D) and
291 NMII enrichment (Fig. 6E-H). Furthermore, we noticed that *Rho1*^{DN}-overexpressing follicle cells
292 shows a floppy and irregular shape, likely due to the disruption of actomyosin contractility and
293 cytoskeleton (Fig. 6C-D and 6G-H). Next, we investigated whether these follicles could still
294 respond to OA-induced follicle rupture. Mature follicles with *Rho1*^{DN} overexpression showed a
295 significant reduction in rupture rate after OA stimulation (Fig. 6I-K). Consistent with this result,
296 females with *Rho1*^{DN} overexpression laid significantly fewer eggs, accumulated more mature
297 follicles in their ovaries after egg laying, and took longer time to ovulate an egg (Fig. 6L-N and
298 SI Appendix, Table S1), indicating that *Rho1*^{DN}-overexpressing females have an ovulation
299 defect. Thus, our data suggest that Rho1 is required for OA-induced follicle rupture *ex vivo* and
300 ovulation *in vivo*.
301 Next, we explored whether Rho1 alone is sufficient to induce follicle rupture and
302 ovulation by overexpressing a constitutively active form of *Rho1* (*Rho1*^{CA}) in mature follicle
303 cells with *47A04-Gal4*. Females with *Rho1*^{CA} overexpression had a severe defect in egg laying,
304 mature follicle retention, and a dramatic increase in ovulation time (Fig. 6L-N and SI Appendix,
305 Table S1), indicating an ovulation defect. To determine the cause of ovulation defect, we
306 examined the ovaries with *Rho1*^{CA} overexpression and discovered that the majority of mature
307 follicles were prematurely ruptured inside the ovaries, while control flies had no mature follicles
308 ruptured inside the ovaries (Fig. 6O-P). This premature follicle rupture could lead to a traffic jam
309 when ovulating oocytes attempted to enter the lateral oviduct that connects to the base of the
310 ovary, since there is only enough space for one oocyte to enter the lateral oviduct at a time. On

311 the other hand, this premature rupture caused by overactivation of Rho1 suggests that Rho1-
312 mediated mechanical force is sufficient to induce follicle rupture. In conclusion, our study
313 demonstrates that OA/OAMB signaling activates Rho1-ROK-actomyosin contraction in the
314 cortex of main-body follicle cells to provide the major mechanical force for follicle rupture
315 during *Drosophila* ovulation (Fig. 7).
316
317 **Discussion**
318 In this study, we investigated the mechanical force required for follicle rupture, a long-
319 lasting question in the ovulation field. Using the powerful genetic tools available in *Drosophila*
320 with pharmacological tools, we clearly demonstrated that OA, the signal for *Drosophila* follicle
321 rupture, induces the cortex accumulation of F-actin and NMII in follicle cells, which contracts
322 and generates mechanical force for follicle rupture during *Drosophila* ovulation (Fig. 7). It is
323 important to note that the contraction mostly occurs at the lateral membrane (potentially in cell-
324 cell junctions) of main-body follicle cells, which likely generate the tension to potentiate the
325 follicle cells to transit from squamous to cuboidal appearance in order to reduce the apical area
326 covering the oocyte (Fig. 7). The activation of MMP2 induced by OA and subsequent breakdown
327 of posterior follicle cells disrupt the balance of this tension, which drives follicle cell
328 morphogenesis and compression toward the anterior dorsal appendage. This model predicts that
329 cell-cell junctions in main-body follicle cells are critical to exert such mechanical force for
330 follicle rupture and will be subjected to future investigation. Together with our previous findings
331 about that OA activates MMP2 in posterior follicle cells for follicle breakdown and NOX in
332 main-body follicle cells for ROS production, our study here introduces a new perspective on

Drosophila ovulation, emphasizing the mechanical force generated in main-body follicle cells by OA signal.

The receptor for mediating OA's effect is likely OAMB, the only α-adrenergic receptor in *Drosophila*. Our previous work has demonstrated that OAMB is critical for OA-induced MMP2 activation, ROS production, and thus follicle rupture (26, 28). Therefore, we focused on OAMB in this study. As expected, *Oamb* mutation significantly reduced OA-induced F-actin, NMII, and Sqh-1P enrichment as well as Rho1 cortex activation (Fig. 3I-N, 5D-H, and SI Appendix, Fig. S5J-N). Our work revealed for the first time the connection between OA signaling and Rho1-actomyosin contraction in non-muscle cells. Since OA has been involved in many biological processes, including lipid and carbohydrate metabolism, arousal level, and learning and memory (64–67), OA-induced Rho1 activation and actomyosin contraction may potentially be involved in these processes, which awaits future investigation.

We did notice that *oamb* mutation did not completely block the OA-induced F-actin, NMII, and Sqh-1P enrichment, consistent with the previous result that *oamb* mutation did not completely block the OA-induced superoxide production and follicle rupture (26, 28). Our previous work showed that *oamb* mRNA is not detectable in *oamb* mutant follicles (26). The recent work from Rohrbach et al. showed that OAMB is the only adrenergic receptor expressed in mature follicle cells (68). This implies that OA may activate another unknown receptor to induce actomyosin contraction in the absence of *oamb*.

We still do not know how OA/OAMB signaling mediates Rho1 activation in the follicle cell cortex. Previous work in *Drosophila* embryo nicely demonstrated that G protein-coupled receptor Mist activates $G_{\alpha 12/13}$ protein Cta (Concertina) to induce RhoGEF2 (Rho guanine

nucleotide exchange factor 2) and subsequent Rho1 activation in apical surface of the embryonic cells with the help of transmembrane protein T48 (69–72). Future investigation will determine whether T48 is expressed in mature follicle cells and thus facilitates Rho1 cortex activation in follicle cells. Further understanding of which G protein downstream of OAMB or any RhoGEF is responsible for transducing OAMB signal to Rho1 activation is of great interest for future research. It is also interesting to find out what causes the differential activation of Rho1 and actomyosin cortex enrichment between main-body and posterior follicle cells, since both receive the OA/OAMB signaling.

In addition to Rho1 and NMII, regulation of actin dynamics in late oogenesis is also poorly understood. Previous studies have shown that F-actin forms basal bundles in follicle cells from stage 10 to 13, which is critical for the final stage of egg elongation (45, 73). Our findings showed that F-actin becomes more dispersed in all follicle cells at stage 14. It is unclear what developmental signal leads to the reorganization of actin cytoskeleton during follicle maturation. Importantly, upon stimulation by OA, F-actin is re-localized to the cortex, primarily in the lateral region of main-body follicle cells. In addition to Rho1, there are two other GTPases (Rac and Cdc42), which are critical for actin polymerization and cell movement. Their role in OA-induced actin polymerization is still unknown and are subject to future investigation.

Actin cytoskeleton is one of the most fundamental and conserved structural components that are known to be involved in countless biological processes across species. In epithelial tissues, it works with non-muscle myosin II to form actomyosin network to controls cell shape, cell migration, tissue morphogenesis (34, 35, 74). This conserved mechanism suggests that the finding of this study may be involved in mammalian ovulation. Several lines of evidence support this prediction. First of all, granulosa cells have a drastic cytoskeleton remodeling and shape

change after LH surge, the signal for mammalian ovulation (14, 15). This cytoskeleton remodeling was shown to be dependent on RhoA, homologous to *Drosophila* Rho1 (14). Second, granulosa cells become highly migratory and exhibit inward migration after LH surge (12, 13, 16). Reducing Fyn, the kinase important for focal adhesion formation and cell migration, in granulosa cells leads to reduced migratory capacity of granulosa cells and ovulation rate (13). Third, while the contraction of smooth muscle cells in the theca layer, triggered by granulosa cell-produced endothelin-2, mediates the constrictions in the basolateral region of the preovulatory follicles, believed to aid in expelling the oocyte during follicle rupture, the granulosa-specific deletion of endothelin-2 in mice only partially inhibits ovulation (5). This is consistent with the previous observation that smooth muscle cells in the theca layer only accounts for minor fraction of the somatic cells in the preovulatory follicles (9). Therefore, additional mechanical force, likely from granulosa cells, is required for efficient ovulation. Future work will be required to decisively determine whether Rho-mediated actomyosin contraction in granulosa cells plays any role in mammalian ovulation like its counterpart in *Drosophila* ovulation.

Materials and Methods

Drosophila genetics and husbandry follow standard procedures. For ectopic expression of RNAi or transgenes with Gal4/UAS system, the progeny were kept in 29 °C to enhance the expression. Except *44E10-Gal4*, *47A04-Gal4* (gifts from Gerald Rubin), *ubi-AniRBD::GFP* (gift from Thomas Lecuit), all the other fly stocks were made in house or acquired from Bloomington Drosophila Stock Center and Vienna Drosophila Resource Center.

All the physiological assays including egg laying, ovulation time, *ex vivo* follicle rupture, *in situ* zymography, and superoxide detection follow standard protocols published previously (26, 75). Immunostaining and microscopy also follow standard procedure (75) except for phalloidin staining, in which case, a master mix of 4% EM-grade paraformaldehyde, Alexa Fluor™ 488 Phalloidin at 1:500 dilution, and 0.1 ug/mL DAPI in 1X PBT was used to fix and stain mature follicles. Laser ablation was carried out using a Zeiss LSM 710. Cortex and cytoplasm intensity measurement is carried out using FIJI. Quantification of follicle volume uses in-house MATLAB scripts.

Detailed materials, protocols and statistical analysis are described in SI Appendix, Supplemental Materials and Methods.

Acknowledgement

We thank Drs Thomas Lecuit, Robert Ward, Gerald Rubin, Allan Spradling, and David Knecht for generously sharing fly lines and reagents; Bloomington Drosophila Stock Center and Vienna Drosophila Resource Center for fly stocks; and Developmental Studies Hybridoma Bank for antibodies. We appreciate UConn Imaging Core facility, the W.M. Keck Facility at the Whitehead Institute, Dr. Yukiko Yamashita lab and Dr. Ruth Lehmann lab for supporting the uses of microscope. The Leica SP8 confocal microscope is supported by an NIH Award (S10OD016435) to Akiko Nishiyama. We appreciate constructive comments from anonymous reviewers. We also thank members of the Sun lab for comments and supports for the manuscript. This project was supported by National Institutes of Health/National Institute of Child Health and Human Development grants (R01-HD086175 and R01-HD097206) to J.S., National Science

Foundation award (2223957) to J.S. and K.H, and National Institutes of Health/National Institute of General Medical Sciences grant (R35-GM144115) to A.C.M.

Competing interests statement

The authors declare no competing financial interests.

References

1. L. L. Espey, J. S. Richards, “Ovulation” in *Physiology of Reproduction*, 3rd Ed., J. D. Neill, Ed. (Academic Press, 2006), pp. 425–474.

2. R. L. Robker, J. D. Hennebold, D. L. Russell, Coordination of Ovulation and Oocyte Maturation: A Good Egg at the Right Time. *Endocrinology* **159**, 3209–3218 (2018).

3. D. M. Duffy, C. Ko, M. Jo, M. Brannstrom, T. E. Curry, Ovulation: Parallels With Inflammatory Processes. *Endocr. Rev.* **40**, 369–416 (2019).

4. C. J. Ko, Y. M. Cho, E. Ham, J. A. Cacioppo, C. J. Park, Endothelin 2: a key player in ovulation and fertility. *Reproduction* **163**, R71–R80 (2022).

5. J. A. Cacioppo, *et al.*, Granulosa cell endothelin-2 expression is fundamental for ovulatory follicle rupture. *Sci. Rep.* **7**, 817 (2017).

6. C. Ko, *et al.*, Endothelin-2 in Ovarian Follicle Rupture. *Endocrinology* **147**, 1770–1779 (2006).

7. G. S. Palanisamy, *et al.*, A Novel Pathway Involving Progesterone Receptor, Endothelin-2, and Endothelin Receptor B Controls Ovulation in Mice. *Mol. Endocrinol.* **20**, 2784–2795 (2006).

8. G. G. Martin, P. Talbot, Drugs that block smooth muscle contraction inhibit in vivo ovulation in hamsters. *J. Exp. Zool.* **216**, 483–491 (1981).

9. G. G. Martin, P. Talbot, The role of follicular smooth muscle cells in hamster ovulation. *J. Exp. Zool.* **216**, 469–482 (1981).

10. P. Talbot, R. S. Chacon, In vitro ovulation of hamster oocytes depends on contraction of follicular smooth muscle cells. *J. Exp. Zool.* **224**, 409–415 (1982).

11. M. Matousek, C. Carati, B. Gannon, M. Brannstrom, Novel method for intrafollicular pressure measurements in the rat ovary: increased intrafollicular pressure after hCG stimulation. *Reproduction* **121**, 307–314 (2001).

12. S. Bianco, *et al.*, The Ovulatory Signal Precipitates LRH-1 Transcriptional Switching Mediated by Differential Chromatin Accessibility. *Cell Rep.* **28**, 2443-2454.e4 (2019).

13. H. Grossman, *et al.*, A novel regulatory pathway in granulosa cells, the LH/human chorionic gonadotropin-microRNA-125a-3p-Fyn pathway, is required for ovulation. *FASEB J.* **29**, 3206–3216 (2015).

14. A. B. Karlsson, *et al.*, Luteinizing Hormone Receptor-Stimulated Progesterone Production by Preovulatory Granulosa Cells Requires Protein Kinase A-Dependent Activation/Dephosphorylation of the Actin Dynamizing Protein Cofilin. *Mol. Endocrinol.* **24**, 1765–1781 (2010).

15. A. BEN-ZE'EV, A. AMSTERDAM, Regulation of Cytoskeletal Protein Organization and Expression in Human Granulosa Cells in Response to Gonadotropin Treatment*. *Endocrinology* **124**, 1033–1041 (1989).

16. C. M. Owen, L. A. Jaffe, Luteinizing hormone stimulates ingression of mural granulosa cells within the mouse preovulatory follicle†. *Biol. Reprod.* ioad142 (2023). https://doi.org/10.1093/biolre/ioad142.

17. S. Matsuzaki, Mechanobiology of the female reproductive system. *Reprod. Med. Biol.* **20**, 371–401 (2021).

18. E. J. Zaniker, E. Babayev, F. E. Duncan, Common mechanisms of physiological and pathological rupture events in biology: novel insights into mammalian ovulation and beyond. *Biol. Rev.* **98**, 1648–1667 (2023).

19. C. Berg, M. Sieber, J. Sun, Finishing the egg. *Genetics* iyad183 (2023). https://doi.org/10.1093/genetics/iyad183.

20. A. C. Spradling, "Developmental genetics of oogenesis" in *The Development of Drosophila Melanogaster*, M. Bate, A. Martinez-Arias, Eds. (Cold Spring Harbor Laboratory Press, 1993), pp. 1–70.

21. T. Roeder, TYRAMINE AND OCTOPAMINE: Ruling Behavior and Metabolism. *Annu. Rev. Entomol.* **50**, 447–477 (2005).

22. S. H. Cole, *et al.*, Two functional but noncomplementing Drosophila tyrosine decarboxylase genes: distinct roles for neural tyramine and octopamine in female fertility. *J Biol Chem* **280**, 14948–55 (2005).

23. H.-G. Lee, C.-S. Seong, Y.-C. Kim, R. L. Davis, K.-A. Han, Octopamine receptor OAMB is required for ovulation in Drosophila melanogaster. *Dev. Biol.* **264**, 179–190 (2003).

24. M. Monastirioti, Distinct octopamine cell population residing in the CNS abdominal ganglion controls ovulation in Drosophila melanogaster. *Dev. Biol.* **264**, 38–49 (2003).

25. M. Monastirioti, C. E. Linn Jr, K. White, Characterization of Drosophila tyramine β-hydroxylase gene and isolation of mutant flies lacking octopamine. *J. Neurosci.* **16**, 3900–3911 (1996).

26. L. D. Deady, J. Sun, A Follicle Rupture Assay Reveals an Essential Role for Follicular Adrenergic Signaling in Drosophila Ovulation. *PLoS Genet* **11**, e1005604 (2015).

27. L. D. Deady, W. Shen, S. A. Mosure, A. C. Spradling, J. Sun, Matrix Metalloproteinase 2 Is Required for Ovulation and Corpus Luteum Formation in Drosophila. *PLoS Genet.* **11**, e1004989 (2015).

28. W. Li, J. F. Young, J. Sun, NADPH oxidase-generated reactive oxygen species in mature follicles are essential for Drosophila ovulation. *Proc. Natl. Acad. Sci.* **115**, 7765–7770 (2018).

29. S. A. Deshpande, *et al.*, Regulation of *Drosophila* oviduct muscle contractility by octopamine. *iScience* **25**, 104697 (2022).

30. W. Luo, *et al.*, Juvenile hormone signaling promotes ovulation and maintains egg shape by inducing expression of extracellular matrix genes. *Proc. Natl. Acad. Sci. U. S. A.* **118**, e2104461118 (2021).

31. C. D. Rubinstein, M. F. Wolfner, Drosophila seminal protein ovulin mediates ovulation through female octopamine neuronal signaling. *Proc. Natl. Acad. Sci.* **110**, 17420–17425 (2013).

32. H.-G. Lee, S. Rohila, K.-A. Han, The Octopamine Receptor OAMB Mediates Ovulation via Ca2+/Calmodulin-Dependent Protein Kinase II in the Drosophila Oviduct Epithelium. *PLOS ONE* **4**, e4716 (2009).

33. E. Rodriguez-Mesa, M. T. Abreu-Blanco, A. E. Rosales-Nieves, S. M. Parkhurst, Developmental expression of Drosophila Wiskott-Aldrich Syndrome family proteins. *Dev. Dyn.* **241**, 608–626 (2012).

34. P. Agarwal, R. Zaidel-Bar, Principles of Actomyosin Regulation *In Vivo*. *Trends Cell Biol.* **29**, 150–163 (2019).

35. D. N. Clarke, A. C. Martin, Actin-based force generation and cell adhesion in tissue morphogenesis. *Curr. Biol.* **31**, R667–R680 (2021).

36. J. Gates, Drosophila egg chamber elongation. *Fly (Austin)* **6**, 213–227 (2012).

37. N. Xu, G. Bagumian, M. Galiano, M. M. Myat, Rho GTPase controls Drosophila salivary gland lumen size through regulation of the actin cytoskeleton and Moesin. *Development* **138**, 5415–5427 (2011).

38. A. G. Szent-Györgyi, The Early History of the Biochemistry of Muscle Contraction. *J. Gen. Physiol.* **123**, 631–641 (2004).

39. M. Vicente-Manzanares, X. Ma, R. S. Adelstein, A. R. Horwitz, Non-muscle myosin II takes centre stage in cell adhesion and migration. *Nat. Rev. Mol. Cell Biol.* **10**, 778–790 (2009).

40. M. Ikebe, D. J. Hartshorne, Phosphorylation of smooth muscle myosin at two distinct sites by myosin light chain kinase. *J. Biol. Chem.* **260**, 10027–10031 (1985).

41. P. Jordan, R. Karess, Myosin Light Chain–activating Phosphorylation Sites Are Required for Oogenesis in Drosophila. *J. Cell Biol.* **139**, 1805–1819 (1997).

42. A. Munjal, T. Lecuit, Actomyosin networks and tissue morphogenesis. *Dev. Camb. Engl.* **141**, 1789–1793 (2014).

43. C. G. Vasquez, S. M. Heissler, N. Billington, J. R. Sellers, A. C. Martin, Drosophila non-muscle myosin II motor activity determines the rate of tissue folding. *eLife* **5**, e20828 (2016).

44. A. Schmidt, L. Li, Z. Lv, S. Yan, J. Großhans, Dia- and Rok-dependent enrichment of capping proteins in a cortical region. *J. Cell Sci.* **134**, jcs258973 (2021).

45. L. He, X. Wang, H. L. Tang, D. J. Montell, Tissue elongation requires oscillating contractions of a basal actomyosin network. *Nat. Cell Biol.* **12**, 1133–1142 (2010).

46. A. C. Martin, B. Goldstein, Apical constriction: themes and variations on a cellular mechanism driving morphogenesis. *Development* **141**, 1987–1998 (2014).

47. J. M. Verboon, S. M. Parkhurst, Rho family GTPase functions in Drosophila epithelial wound repair. *Small GTPases* **6**, 28–35 (2015).

48. G. Aranjuez, A. Burtscher, K. Sawant, P. Majumder, J. A. McDonald, Dynamic myosin activation promotes collective morphology and migration by locally balancing oppositional forces from surrounding tissue. *Mol. Biol. Cell* **27**, 1898–1910 (2016).

49. A. M. Gabbert, *et al.*, Septins regulate border cell surface geometry, shape, and motility downstream of Rho in Drosophila. *Dev. Cell* **58**, 1399-1413.e5 (2023).

50. M. C. Lamb, *et al.*, Fascin limits Myosin activity within Drosophila border cells to control substrate stiffness and promote migration. *eLife* **10**, e69836 (2021).

51. P. Majumder, G. Aranjuez, J. Amick, J. A. McDonald, Par-1 Controls Myosin-II Activity through Myosin Phosphatase to Regulate Border Cell Migration. *Curr. Biol.* **22**, 363–372 (2012).

52. J. Imran Alsous, *et al.*, Dynamics of hydraulic and contractile wave-mediated fluid transport during Drosophila oogenesis. *Proc. Natl. Acad. Sci. U. S. A.* **118**, e2019749118 (2021).

53. W. E. Theurkauf, T. I. Hazelrigg, In vivo analyses of cytoplasmic transport and cytoskeletal organization during Drosophila oogenesis: characterization of a multi-step anterior localization pathway. *Development* **125**, 3655–3666 (1998).

54. A. Popkova, M. Rauzi, X. Wang, Cellular and Supracellular Planar Polarity: A Multiscale Cue to Elongate the Drosophila Egg Chamber. *Front. Cell Dev. Biol.* **9**, 645235 (2021).

55. X. Qin, *et al.*, Cell-matrix adhesion and cell-cell adhesion differentially control basal myosin oscillation and Drosophila egg chamber elongation. *Nat. Commun.* **8**, 14708 (2017).

56. S. Vlachos, N. Harden, Genetic Evidence for Antagonism Between Pak Protein Kinase and Rho1 Small GTPase Signaling in Regulation of the Actin Cytoskeleton During Drosophila Oogenesis. *Genetics* **187**, 501–512 (2011).

57. D. Drummond-Barbosa, A. C. Spradling, Alpha-endosulfine, a potential regulator of insulin secretion, is required for adult tissue growth control in Drosophila. *Dev. Biol.* **266**, 310–321 (2004).

58. C. G. Winter, *et al.*, Drosophila Rho-associated kinase (Drok) links Frizzled-mediated planar cell polarity signaling to the actin cytoskeleton. *Cell* **105**, 81–91 (2001).

59. L. Zhang, R. E. Ward, Distinct tissue distributions and subcellular localizations of differently phosphorylated forms of the myosin regulatory light chain in Drosophila. *Gene Expr. Patterns* **11**, 93–104 (2011).

60. M. Uehata, *et al.*, Calcium sensitization of smooth muscle mediated by a Rho-associated protein kinase in hypertension. *Nature* **389**, 990–994 (1997).

61. E. Sahai, C. J. Marshall, ROCK and Dia have opposing effects on adherens junctions downstream of Rho. *Nat. Cell Biol.* **4**, 408–415 (2002).

62. M. S. Hutson, *et al.*, Forces for morphogenesis investigated with laser microsurgery and quantitative modeling. *Science* **300**, 145–149 (2003).

63. A. Munjal, J.-M. Philippe, E. Munro, T. Lecuit, A self-organized biomechanical network drives shape changes during tissue morphogenesis. *Nature* **524**, 351–355 (2015).

64. C. J. Burke, *et al.*, Layered reward signalling through octopamine and dopamine in Drosophila. *Nature* **492**, 433–437 (2012).

65. R. Erion, J. R. DiAngelo, A. Crocker, A. Sehgal, Interaction between sleep and metabolism in Drosophila with altered octopamine signaling. *J. Biol. Chem.* **287**, 32406–32414 (2012).

66. P. D. Evans, B. Maqueira, Insect octopamine receptors: a new classification scheme based on studies of cloned Drosophila G-protein coupled receptors. *Invertebr. Neurosci. IN* **5**, 111–118 (2005).

67. J. Luo, O. V. Lushchak, P. Goergen, M. J. Williams, D. R. Nässel, Drosophila insulin-producing cells are differentially modulated by serotonin and octopamine receptors and affect social behavior. *PloS One* **9**, e99732 (2014).

68. E. W. Rohrbach, E. M. Knapp, S. A. Deshpande, D. E. Krantz, Expression and potential regulatory functions of Drosophila octopamine receptors in the female reproductive tract. *G3 GenesGenomesGenetics* **14**, jkae012 (2024).

69. V. Kölsch, T. Seher, G. J. Fernandez-Ballester, L. Serrano, M. Leptin, Control of Drosophila gastrulation by apical localization of adherens junctions and RhoGEF2. *Science* **315**, 384–386 (2007).

70. A. J. Manning, K. A. Peters, M. Peifer, S. L. Rogers, Regulation of epithelial morphogenesis by the G protein-coupled receptor mist and its ligand fog. *Sci. Signal.* **6**, ra98 (2013).

71. K. K. Nikolaidou, K. Barrett, A Rho GTPase signaling pathway is used reiteratively in epithelial folding and potentially selects the outcome of Rho activation. *Curr. Biol. CB* **14**, 1822–1826 (2004).

72. S. Parks, E. Wieschaus, The Drosophila gastrulation gene concertina encodes a G alpha-like protein. *Cell* **64**, 447–458 (1991).

73. G. Wahlström, H.-L. Norokorpi, T. I. Heino, Drosophila alpha-actinin in ovarian follicle cells is regulated by EGFR and Dpp signalling and required for cytoskeletal remodelling. *Mech. Dev.* **123**, 801–818 (2006).

74. T. Lecuit, P.-F. Lenne, Cell surface mechanics and the control of cell shape, tissue patterns and morphogenesis. *Nat. Rev. Mol. Cell Biol.* **8**, 633–644 (2007).

75. R. Oramas, E. M. Knapp, B. Zeng, J. Sun, The bHLH-PAS transcriptional complex Sim:Tgo plays active roles in late oogenesis to promote follicle maturation and ovulation. *Dev. Camb. Engl.* **150**, dev201566 (2023).

Figure legends

Figure 1. OA-induced follicle swelling is not required for follicle rupture. (A) Representative images show a mature follicle before and after follicle rupture. Follicle cells are marked by *44E10-Gal4* driving *UAS-RG6* expression (*44E10>RG6*, shown in red). Yellow arrows indicate the length of the follicle-cell layer along the anterior-posterior (A-P) axis. **(B-C)** Quantification of the length (B) and the compression ratio (C) of the follicle-cell layer along the A-P axis before and after rupture. **(D-F)** Time-lapse images show mature follicles in control medium without OA (D) or with OA (E), or in hypertonic medium with OA (F). Follicle cells are marked with *47A04-Gal4* driving *UAS-RG6* (*47A04>RG6*) expression in white. Yellow arrows indicate dented/wrinkled surface on follicles. Scale bars: 100 μm**. (G-H)** Quantification of the change of mature follicle volume with or without OA treatment in control or hypertonic medium. The volume is normalized to the beginning time point. The final volume change after a 30-minute treatment is summarized in (H), and the number of mature follicles analyzed is indicated in

brackets. Error bars are standard deviation (SD) **(I-J)** Representative images show mature follicles after a three-hour treatment with OA in control (I) and hypertonic (J) medium. Follicle cells are marked by *47A04>RG6* in red, and the bright-field image is pseudo-colored in cyan. Yellow arrowheads indicate ruptured follicles. **(K)** Quantification of OA-induced follicle rupture. The number of mature follicles is in brackets. ***P<0.001, *P<0.05, ns = not significant.

Figure 2. Pharmacological disruption of actin polymerization prevents OA-induced follicle rupture without affecting MMP2 activation and superoxide production. (A-F) Representative images show mature follicles treated with ethanol (A and C), colchicine (20 μg/ml, B), latrunculin A (1 μg/ml, D), DMSO (E), or cytochalasin D (1 μg/ml, F) for 30 minutes followed by OA stimulation for three hours. Follicle cells are marked by *47A04>RG6* in red, and bright-field images are pseudo-colored in cyan. Yellow arrowheads marked the ruptured follicles. **(G)** Quantification of OA-induced follicle rupture after treatment with a variety of compounds as in (A-F). The number of mature follicles is in brackets. **(H-K)** Representative images show mature follicles with gelatinase activity (indicated by gelatin-fluorescein in green) without (H) or with OA (I-K) treatment for three hours. Mature follicles were either treated with DMSO (H-I), cytochalasin D (1 μg/ml, J), or latrunculin A (1 μg/ml, K). Follicle cells are marked by *47A04>RG6* (red). Follicles with posterior fluorescein signal are clustered toward the upper panel. **(L)** Quantification of OA-induced posterior MMP activity after treatment with chemicals as in H-K. The number of mature follicles is in brackets. **(M)** Quantification of OA-induced superoxide production indicated by L-012-emitted relative luminescence unit (RLU).

Mature follicles were treated with DMSO, cytochalasin D (1 μg/mL) or latrunculin A (1μg/mL) for 30 min before OA stimulation. Also see Figure S1D. ****P<0.0001, ns = not significant.

Figure 3. OA/OAMB induces the cortex enrichment of actomyosin in main-body follicle cells. (A-C) Representative images show F-actin (marked by phalloidin staining in white) in mature follicles immediately after isolation (A), or cultured for 30 minutes without (B) and with (C) OA. Yellow arrows demarcate the border between main-body and posterior follicle cells. **(D)** Quantification of the ratio of F-actin intensity between the cortex and the cytoplasm of main-body follicle cells with or without OA treatment. Each OA+ group was compared to its corresponding OA- group for statistical analysis. **(E-G)** Representative images show Sqh::GFP expression (white) in mature follicles immediately after isolation (E), or cultured for 30 minutes without (F) or with (G) OA. Yellow arrows demarcate the border between main-body and posterior follicle cells. **(H)** Quantification of the ratio of Sqh::GFP intensity between the cortex and the cytoplasm of main-body follicle cells with or without OA treatment. Each OA+ group was compared to its corresponding OA- group for statistical analysis. **(I-K)** Representative images show F-actin (white in I-J) in mature follicles treated with OA for 30 minutes. Mature follicles are from control (I) or *Oamb* mutant (J) females. Quantification of the ratio of F-actin intensity between the cortex and the cytoplasm in main-body follicle cells is shown in K. **(L-N)** Representative images show Sqh::GFP expression (white in L-M) in mature follicles isolated from control (L) and *Oamb* mutant (M) females and treated with OA for 30 minutes. Quantification of the ratio of Sqh::GFP intensity between the cortex and the cytoplasm of main-body follicle cells is shown in N. Data are mean ± s.e.m. (D, H, K, N). ****P<0.0001, ns = not significant.

Figure 4. Rok regulates actomyosin contraction and is required for follicle rupture. (A-L) Representative images show Sqh-1P antibody staining (white in A-D), Sqh::GFP (white in E-H), and F-actin (phalloidin staining, white in I-L) in mature follicles after a 30-minute culture without (A, C, E, G, I, and K) or with (B, D, F, H, J, and L) OA stimulation. Mature follicles were pretreated with either control (A-B, E-F, I-J) or 100 μM Y-27632 (C-D, G-H, K-L). Also see Figure S4. **(M-R')** Time-lapse images show Sqh::GFP (white in M-R) and cell membrane (white in M'-R') dynamics before and after laser ablation. The laser ablation sites are indicated by green arrowheads, and the adjacent tri-cellular junctions are marked with yellow asterisks. Mature follicles were pretreated with control (M-O) or 100 μM Y-27632 (P-R) for 15 minutes followed by OA stimulation for 30 minutes before laser ablation. **(S)** Quantification of initial recoil velocity of the adjacent tricellular junctions within 12 seconds after laser ablation in control and Y-27632-treated follicles. **(T-U)** Representative images show mature follicles treated with control (T) or Y-27632 (100 μM, U) for 30 minutes followed by OA stimulation for three hours. Follicle cells are marked by *47A04>RG6* in red, and bright-field images are pseudo-colored in cyan. Yellow arrowheads mark the ruptured follicles, and the dotted circles indicate the breakdown of posterior follicle wall. **(V)** Dose-dependent inhibition of OA-induced follicle rupture by Y-27632. The number of mature follicles is in brackets. ***P<0.001.

Figure 5. OA/OAMB induces Rho1 activation at the follicle cell cortex. (A-B) Representative images show Ani-RBD::GFP (white in A-B) in mature follicles after a 30-minute culture without (A) or with (B) OA. Yellow arrowheads demarcate the border between main-body and posterior follicle cells. **(C)** Quantification of mature follicles with cortex-enriched Ani-

693 RBD::GFP (as in B) with or without OA stimulation. We quantified the number of follicles
694 exhibiting the clear cortex enrichment pattern in over 50% of all follicle cells, instead of
695 assessing the GFP intensity. The number of follicles counted is shown in brackets above each
696 bar. Each OA+ group was compared to its corresponding OA- group for statistical analysis. **(D-**
697 **G)** Representative images show Ani-RBD::GFP expression (white in D-G) in mature follicles
698 from control (D-E) and *Oamb* mutant (F-G) females and treated without (D, F) or with (E, G)
699 OA for 30 minutes. **(H)** Quantification of the ratio of Ani-RBD::GFP intensity between the
700 cortex and the cytoplasm of main-body follicle cells with or without OA treatment. Each OA+
701 group was compared to its corresponding OA- group for statistical analysis. Data are mean ±
702 s.e.m. (H). ****P<0.0001, ***P<0.001, **P<0.01.
703
704 **Figure 6. Rho1 is required and sufficient for follicle rupture/ovulation**. **(A-H)** Representative
705 images show F-actin (white in A-D) and Sqh::GFP (white in E-H) in mature follicles cultured for
706 30 minutes without (A, C, E, G) or with (B, D, F, H) OA. Mature follicles were isolated from
707 control females (A-B, E-F) or females with *47A04-Gal4* driving *UAS-Rho1*^{DN} expression (C-D,
708 G-H). **(I-K)** Representative images show mature follicles from control (I) or Rho1DN females
709 and cultured for three hours with OA. Follicle cells are marked by *47A04>RFP* in red, and the
710 bright-field image is pseudo-colored in cyan. Yellow arrowheads indicate ruptured follicles.
711 Quantification of ruptured follicles is shown in (K). The number of mature follicles is in
712 brackets. **(L-N)** Quantification of egg laying capacity (L), mature follicles remained in the ovary
713 after egg laying (M), and the egg laying time (N) in females of control or overexpression of
714 *Rho1*^{DN} or *Rho1*^{CA} driven by *47A04-Gal4*. Also see table S1. **(O-P)** Representative images show

ovarioles from control (O) and *Rho1*^{CA}-overexpressing (P) females. White asterisks indicate pre-ruptured follicles inside the ovary. Mature follicle cells are marked by *47A04>RFP* in red, green autofluorescence from eggshell is in green, and DAPI is used to mark cell nuclei in blue. ***P<0.001.

Figure 7. Schematics of a novel OA-induced contraction pathway in *Drosophila* follicle rupture. Before a mature follicle is exposed to OA, it is dehydrated and actomyosin is located sporadically in follicle cells whose shapes are squamous. Once it is stimulated with OA (rupture has not yet been initiated), the follicle is rehydrated; Rho1 activity, F-actin and NMII are enriched around the cortex along the lateral membrane in order to prepare contraction leading to the follicle rupture. Then, with the breakdown of posterior tip of the mature follicle by MMP2 (Deady et al., 2015), we expect to see that mechanical force that is generated by Rho1-actomyosin contraction will cause the shape of the follicle cells to be more cuboidal and ultimately compress the whole follicle cell layer at the dorsal appendage site. This phenomenon will display the completion of follicle rupture. The signaling mechanism explains that when OA (pink) binds to OAMB (purple), active Rho1 (yellow) is enriched in the cortex, as well as NMII (blue) and F-actin (orange), which will lead to the follicle rupture. (CE = cortex enrichment)

Fig 1

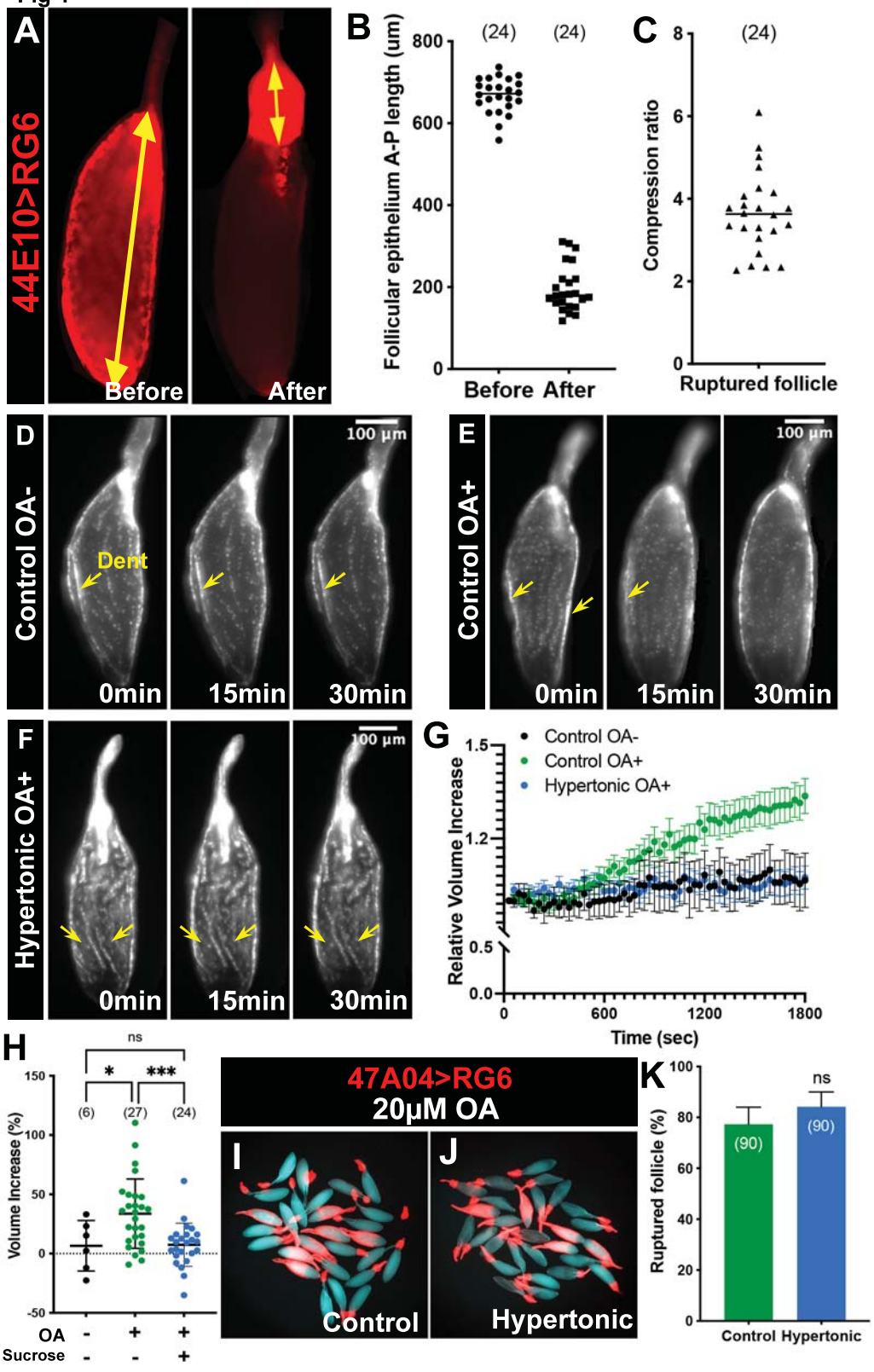
A
44E10>RG6
Before
After
B
Follicular epithelium A-P length (um)
800
600
400
200
0
(24)
(24)
Before
After
C
Compression ratio
8
6
4
2
0
(24)
Ruptured follicle
D
Control OA-
Dent
100 µm
0min
15min
30min
E
Control OA+
100 µm
0min
15min
30min
F
Hypertonic OA+
100 µm
0min
15min
30min
G
Control OA-
Control OA+
Hypertonic OA+
Relative Volume Increase
1.5
1.2
0.5
0.0
0
600
1200
1800
Time (sec)
H
ns
*
***
(6)
(27)
(24)
Volume Increase (%)
150
100
50
0
-50
OA - + +
Sucrose - - +
47A04>RG6
20µM OA
I
Control
J
Hypertonic
K
Ruptured follicle (%)
100
80
60
40
20
0
ns
(90)
(90)
Control
Hypertonic

Fig. 2

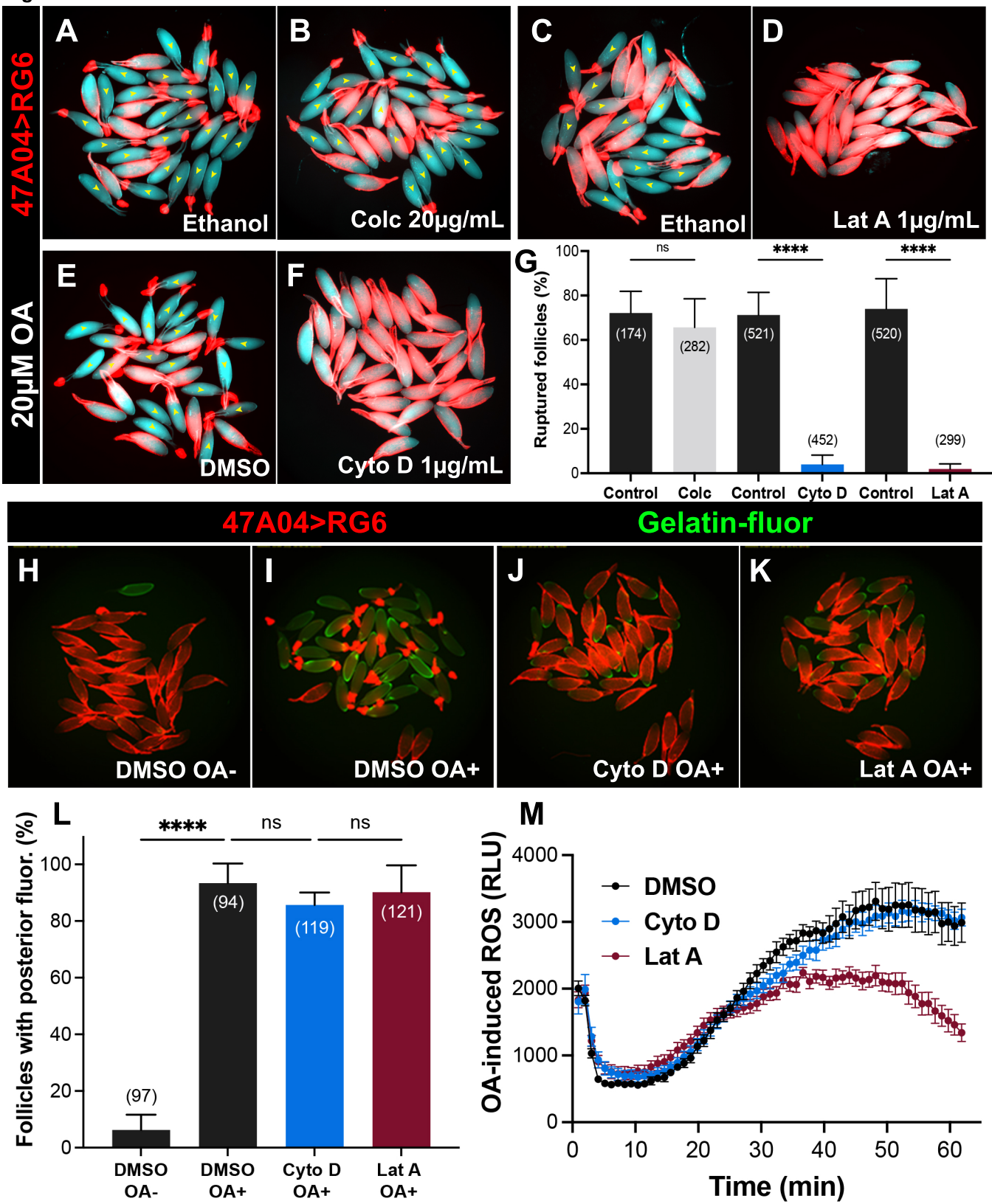
47A04>RG6
20µM OA
A
Ethanol
B
Colc 20µg/mL
C
Ethanol
D
Lat A 1µg/mL
E
DMSO
F
Cyto D 1µg/mL
G
Ruptured follicles (%)
ns
****
****
(174)
(282)
(521)
(452)
(520)
(299)
Control
Colc
Control
Cyto D
Control
Lat A
47A04>RG6
Gelatin-fluor
H
DMSO OA-
I
DMSO OA+
J
Cyto D OA+
K
Lat A OA+
L
Follicles with posterior fluor. (%)
****
ns
ns
(97)
(94)
(119)
(121)
DMSO OA-
DMSO OA+
Cyto D OA+
Lat A OA+
M
OA-induced ROS (RLU)
DMSO
Cyto D
Lat A
Time (min)

Fig. 3

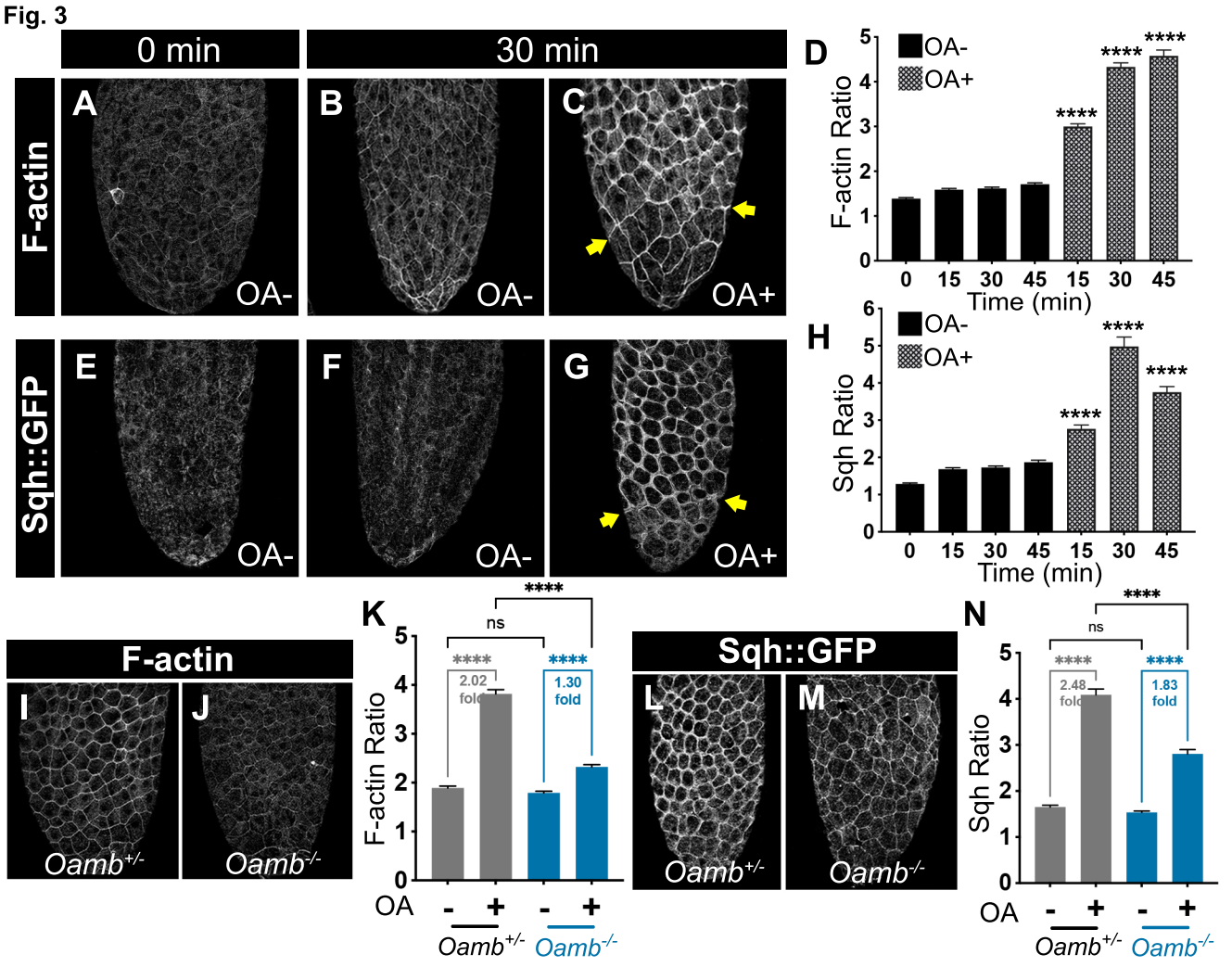
0 min
30 min
F-actin
A
B
C
OA-
OA-
OA+
D
OA-
OA+
F-actin Ratio
****
****
****
0 15 30 45 15 30 45
Time (min)
Sqh::GFP
E
F
G
OA-
OA-
OA+
H
OA-
OA+
Sqh Ratio
****
****
****
0 15 30 45 15 30 45
Time (min)
F-actin
I
J
Oamb+/-
Oamb-/-
K
****
ns
****
F-actin Ratio
2.02 fold
1.30 fold
OA - + - +
Oamb+/-
Oamb-/-
Sqh::GFP
L
M
Oamb+/-
Oamb-/-
N
****
ns
****
Sqh Ratio
2.48 fold
1.83 fold
OA - + - +
Oamb+/-
Oamb-/-

Fig. 4

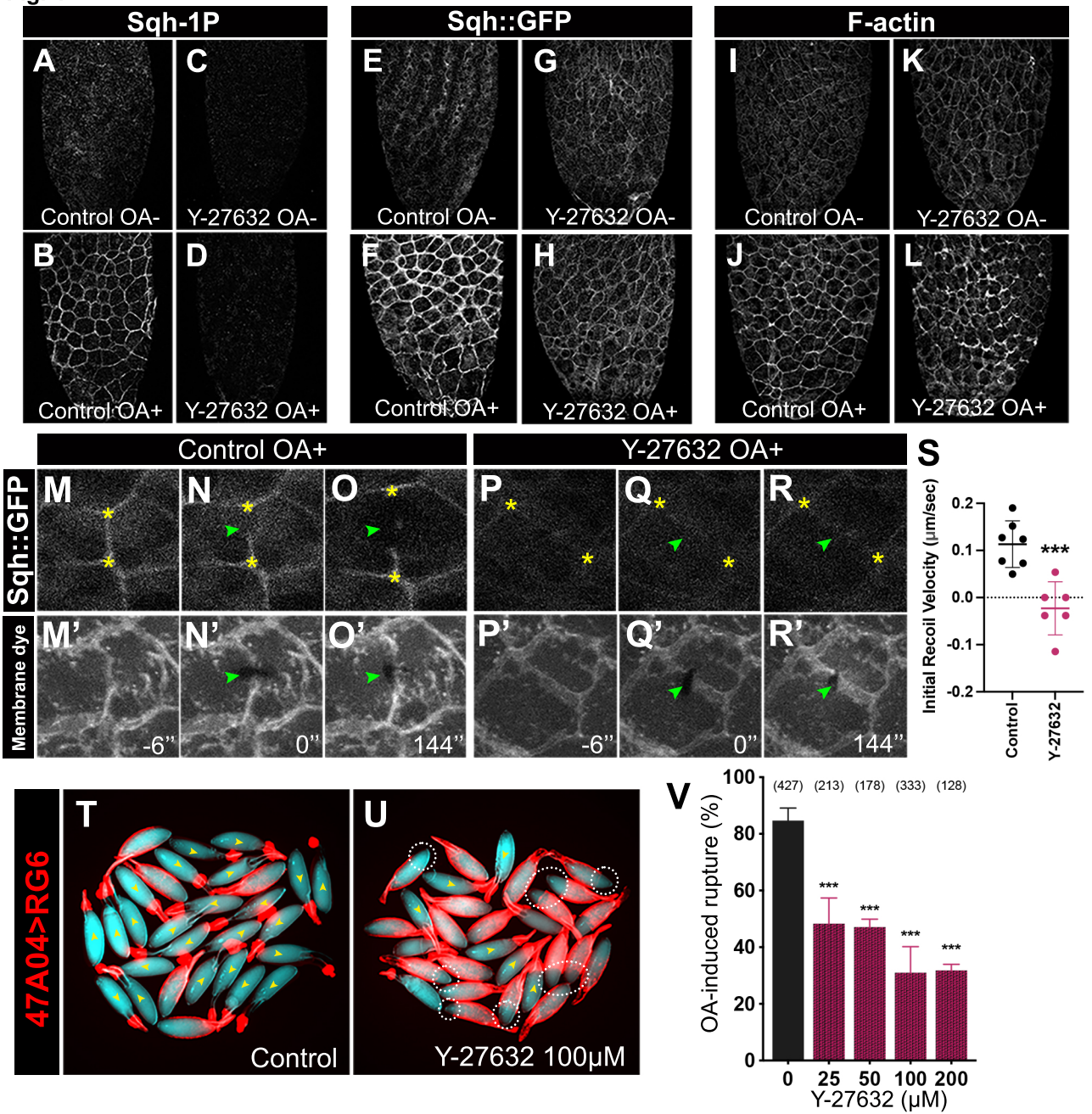
Sqh-1P
Sqh::GFP
F-actin
A
C
E
G
I
K
Control OA-
Y-27632 OA-
Control OA-
Y-27632 OA-
Control OA-
Y-27632 OA-
B
D
F
H
J
L
Control OA+
Y-27632 OA+
Control OA+
Y-27632 OA+
Control OA+
Y-27632 OA+
Sqh::GFP
Membrane dye
M
N
O
P
Q
R
M'
N'
O'
P'
Q'
R'
-6"
0"
144"
-6"
0"
144"
S
Initial Recoil Velocity (µm/sec)
0.2
0.1
0.0
-0.1
-0.2
***
Control
Y-27632
47A04>RG6
T
U
Control
Y-27632 100µM
V
OA-induced rupture (%)
100
80
60
40
20
0
(427)
(213)
(178)
(333)
(128)
***
***
***
***
0
25
50
100
200
Y-27632 (µM)

Fig. 5

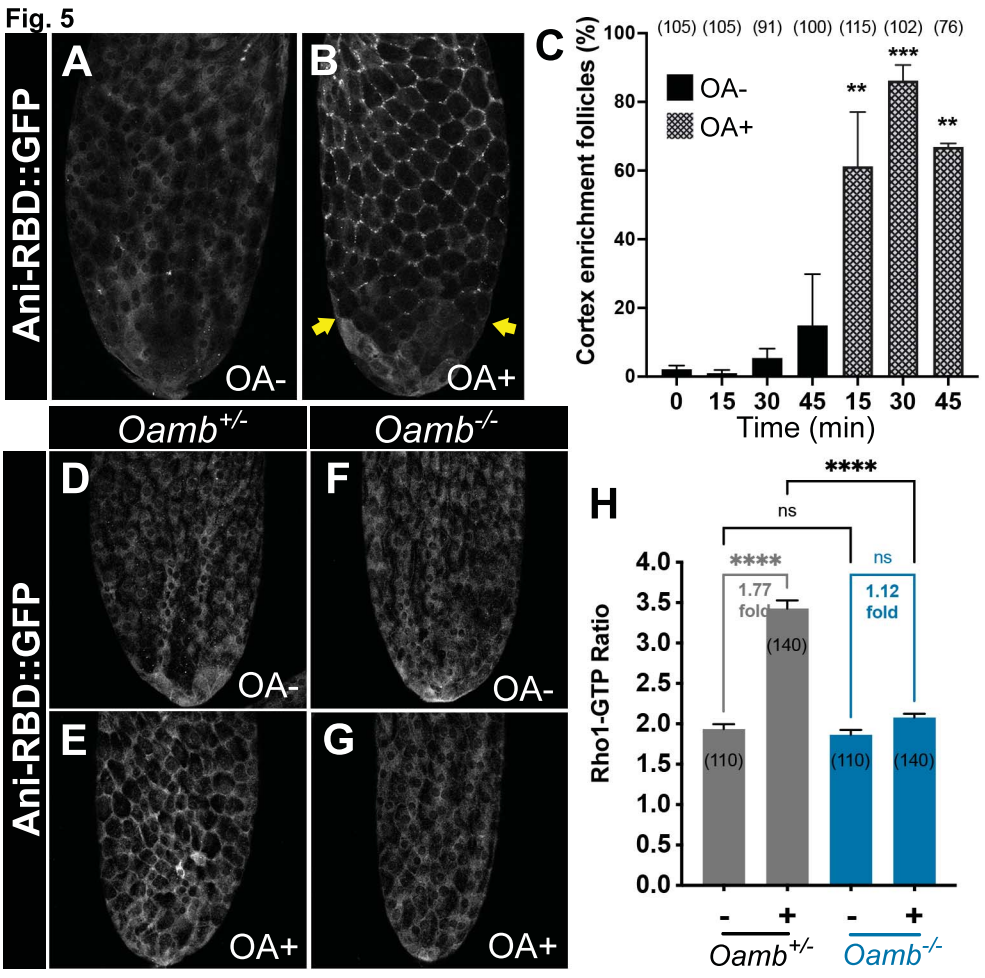
A
B
Ani-RBD::GFP
OA-
OA+
C
(105) (105) (91) (100) (115) (102) (76)
Cortex enrichment follicles (%)
OA-
OA+
0 15 30 45 15 30 45
Time (min)
Oamb+/-
Oamb-/-
D
F
E
G
H
Rho1-GTP Ratio
ns
****
1.77 fold
1.12 fold
(110)
(140)
Oamb+/-
Oamb-/-

Fig. 6

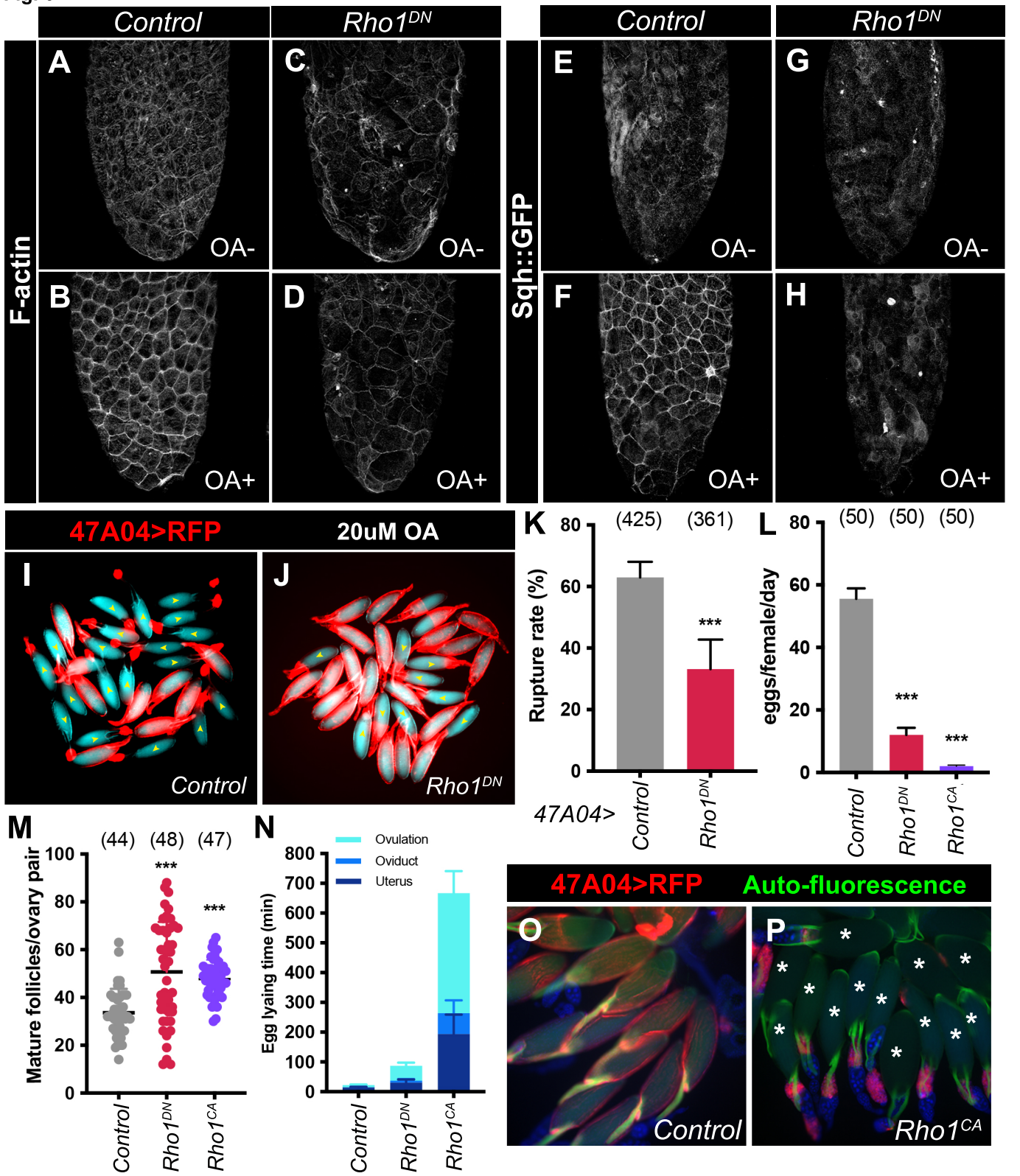
Control
Rho1DN
Control
Rho1DN
F-actin
Sqh::GFP
A
B
C
D
E
F
G
H
OA-
OA+
47A04>RFP
20uM OA
I
J
Control
Rho1DN
K
(425)
(361)
Rupture rate (%)
***
47A04>
Control
Rho1DN
L
(50)
(50)
(50)
eggs/female/day
***
***
Control
Rho1DN
Rho1CA
M
(44)
(48)
(47)
Mature follicles/ovary pair
***
***
Control
Rho1DN
Rho1CA
N
Ovulation
Oviduct
Uterus
Egg lyaing time (min)
Control
Rho1DN
Rho1CA
47A04>RFP
Auto-fluorescence
O
P
Control
Rho1CA

Fig.7

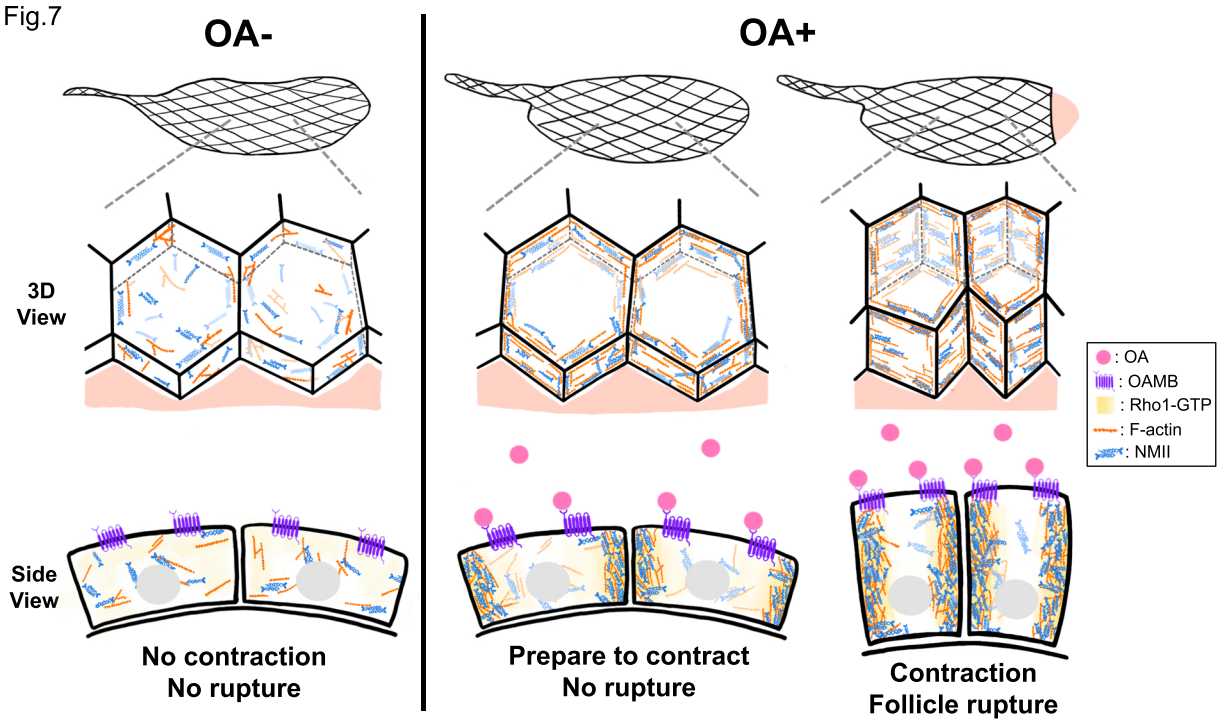
OA-
OA+
3D View
Side View
: OA
: OAMB
: Rho1-GTP
: F-actin
: NMII
No contraction
No rupture
Prepare to contract
No rupture
Contraction
Follicle rupture

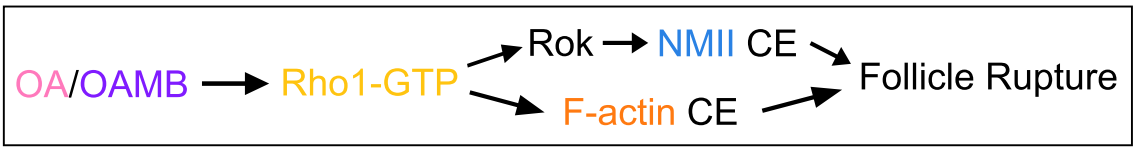
OA/OAMB
Rho1-GTP
Rok
NMII CE
F-actin CE
Follicle Rupture